

05

Study of Hyperfine Interaction Parameters and Magnetic State in Fe–Al–B Ternary Alloys by DFT Method

© A.F. Abdullin, E.V. Voronina

Kazan Federal University,
Kazan, Tatarstan, Russia

E-mail: ayazik@bk.ru

Received September 8, 2025

Revised September 8, 2025

Accepted November 12, 2025

The results of quantum-mechanical calculations of hyperfine interaction parameters (hyperfine fields and isomer shifts at the ^{57}Fe nucleus) in Fe–Al–B ternary alloys are presented. It is shown that substituting iron atoms with aluminum or boron atoms in the first coordination sphere of the Fe atom leads to a decrease in the hyperfine magnetic field by approximately 2.7 T per atom and an increase in the isomer shift by 0.02 mm/s per atom. The effect of substitutions in more distant coordination shells generally requires further analysis of the local atomic structure. The analysis of contributions to the ^{57}Fe hyperfine magnetic field from core and valence electrons revealed a proportionality between the hyperfine magnetic field and the magnetic moment of the core d -electrons, with a coefficient of about $12.4 \text{ T}/\mu_{\text{B}}$, without a pronounced correlation with the contribution from valence electrons. Energetically stable periodic structures with boron atoms in interstitial positions are considered on the example of the $\text{Fe}_{11}\text{Al}_5\text{B}$ and $\text{Fe}_{12}\text{Al}_4\text{B}$ systems. The obtained results have practical significance for the interpretation of Mössbauer spectra.

Keywords: DFT calculations, Fe–Al–B ternary alloys, hyperfine interactions, local atomic structure.

DOI: 10.61011/PSS.2025.11.62973.1k-25

1. Introduction

Ordered binary and multi-component intermetallic compounds based on Fe–Al system are of great interest both due to their potential technological use [1,2] and as model systems to study magnetic phenomena. In particular, materials based on Fe–Al with boron additives are critical for technical applications due to its magnetic elastic properties and are promising as materials for sensors and actuators [3,4]. One of the most important features of binary Fe–Al systems is pronounced dependence of their magnetic behavior on the structure and content of Al. It is known that even small changes of Al concentration (starting from 28–30 at.%) result in pronounced changes of the alloy magnetic state [5,6]. To find out how the features of the structure influence the magnetic state, and also to interpret the experimental observations for the binary Fe–Al system, many theoretical studies of electron and magnetic structure were carried out based on the first principles [7–12]. The long-standing puzzle of the vanishing ferromagnetism in Fe–Al alloys with content of Al > 30 at.% is known from the middle of the 60s of the last century [13] was resolved in the neutron diffraction studies by Noakes et al. [14]. In the experiments on single-crystal aluminides with Al content from 34 to 43 at.%, spatial correlations of the magnetic moment were found, and the analysis indicated that they could be interpreted as static, incommensurate spin structures — e.g., spin-density waves (SDW). However, so far both the origin and the conditions of such magnetic structures existence

are unclear, and even their identification remains a complex experimental objective. Besides, the cause for existence of static, incommensurate spin structures only in the specified concentration range remains unclarified.

In our experimental papers [15–17] we used magnetometry and Mössbauer spectroscopy (MS) to study the effect of addition of Ga or B — isoelectronic analogues of aluminum (also Sn) — on the evolution of the $\text{Fe}_{65}\text{Al}_{35}$ binary alloy magnetic state. For example, it was shown that the addition of more than 10 at.% boron causes phase separation of the alloy and precipitation of a metastable phase within the Fe–Al lattice, which is expected to enhance certain mechanical and magnetoelastic properties. To interpret the magnetic microstructure of ternary systems (Fe–Al– M , $M = \text{Ga}, \text{B}, \text{Sn}$), the information on local parameters of hyperfine interactions (HFI) and magnetic moments obtained independently, using quantum-mechanical calculations, turned out to be rather in demand. For the ternary system of Fe–Al–B the available theoretical studies are quite scarce. They study the electron structure, elastic properties [18], conditions for stabilization of various defects [19], energy performance of boron atoms impurities in B2-FeAl intermetallic compound [20]. Some aspects of noncollinear magnetism in ternary Fe–Al–B alloys were studied in our previous paper [21], where quantum-mechanical calculations found high sensitivity of magnetic ordering to concentration of sp -elements and local arrangement of atoms in the lattice. Addition of a small quantity of boron causes a change in the energy balance of the system, as a result of which ferromagnetic ordering

becomes more beneficial from the energy point of view compared to the spin-spiral structure. Besides, it is very interesting how the specific positions of boron atoms within the crystal lattice affect the magnetic properties of the alloy. This question has remained understudied so far is one of the objectives of this paper.

The presented objective is dedicated to the calculations of the electronic structure within the density functional theory (DFT), magnetic moments and HFI parameters (namely, hyperfine magnetic field (HMF) in ^{57}Fe nucleus and isomer shift δ) for Fe–Al and Fe–Al–B systems with a focus on the cells with the composition close to $\text{Fe}_{65}\text{Al}_{30}\text{B}_5$. For the ternary system, the contributions from core electrons and valence electrons to the HMF ^{57}Fe have been analyzed. Additionally, we examined unit cells in which a boron atom occupies the $D0_3$ interstitial sites of the superlattice and analyzed the resulting changes in the HFI parameters. This article is a part of a comprehensive study of ternary alloys (including Fe–Al–B), that combines quantum-mechanical calculations with experimental data. This will allow a clearer elucidation of the relationships among chemical composition, local structure, and the magnetic properties of Fe–Al-based binary and ternary alloys.

2. Calculation details

Theoretical quantum-mechanical calculations of local magnetic characteristics were carried out on the basis of the density functional theory using WIEN2k software package [22–24]. The exchange-correlation potential was taken into account within the generalized gradient approximation (GGA) with PBE parameterization [24]. Wave functions, charge density and potential were expanded in spherical harmonics inside non-overlapping (*muffin-tin*) atomic spheres of radius R_{mt} and in plane waves within the interstitial region of the unit cell. Radii of *muffin-tin* spheres were set as equal to 2.00 arb. un. for all atoms, except those occupying interstitial sites. Inside the atomic spheres the decomposition of electron wave functions was limited to number $l_{\text{max}} = 10$, and the potential was expanded into spherical harmonics to $l = 4$. In the interstitial area the wave functions were presented as plane waves with the maximum cut vector K_{max} , specified by ratio $R_{\text{mt}} \cdot K_{\text{max}} = 7$. The charge density was expanded into the Fourier's series to $G_{\text{max}} = 20 \text{ Ry}^{1/2}$. In the irreducible part of the Brillouin's zone the number of k -points was chosen to provide for the convergence of full energy of the unit cell with the accuracy of up to 0.1 meV — $16 \times 16 \times 16$ k -points. When necessary, the interatomic distances were relaxed until the forces acting on the atoms approached zero.

Multiple unit cells were analyzed, such as: FeAl_{15} , $\text{Fe}_2\text{Al}_{14}$, $\text{Fe}_8\text{Al}_4\text{B}_4$, $\text{Fe}_8\text{Al}_5\text{B}_3$, $\text{Fe}_8\text{Al}_6\text{B}_2$, $\text{Fe}_8\text{Al}_7\text{B}$, Fe_8Al_8 , Fe_9Al_7 , $\text{Fe}_9\text{Al}_6\text{B}$, $\text{Fe}_{10}\text{Al}_5\text{B}$, $\text{Fe}_{11}\text{Al}_5$, $\text{Fe}_{12}\text{Al}_4$, $\text{Fe}_{12}\text{Al}_2\text{B}_2$, Fe_{13}B_3 , $\text{Fe}_{13}\text{Al}_2$, Fe_{14}B_2 , Fe_{15}B , Fe_{15}Al and many others. Concentration of aluminum and boron atoms varied in a wide range from 0 to 93.75 at.%.

3. Results and discussion

3.1. Calculations of hyperfine interactions parameters

Quantum-mechanical calculations were performed using models based on crystallographic unit cells containing 16 atoms, with the Fe, Al, and B compositions varied. This approach enabled a detailed study of how different atomic species and their arrangement within the unit cell (up to the fourth coordination shell) affect the HFI parameters. Special attention was paid to analysis of HFI parameters, namely: HMF, isomer shifts as well as magnetic moments of Fe atoms — because understanding how these quantities evolve provides deeper insight into the electronic and magnetic structure of Fe–Al–B ternary alloys.

Distribution of Al and B atoms in the coordination shells around the central iron atom provides substantial affects on the HFI parameters. Analysis of the calculated HFI parameters showed that the number and arrangement of atoms in the first coordination shell are the most significant factors (Figure 1, *a*). Dependence of the calculated HMF B_{hf} on the number of sp -elements (Al/B) located in I coordination shell of Fe atom can be approximated by a linear function (black line). Replacement of one Fe atom for sp -element in I coordination shell causes HMF reduction by approximately 2.7 T. If you consider a binary system — only Al atoms in I coordination shell — (they are marked as filled circles on the graph), the slope of the approximating line varies slightly (red line) — the reduction is approximately 2.4 T, which is in good agreement with the available experimental data [13]. Reduction of the local HMF in ^{57}Fe nucleus when iron is replaced with aluminum or boron is due to the change in the electron density and magnetic moment of iron atom. This change happens due to redistribution of d -electrons, which modifies the exchange interactions, and, as a result, the HMF value.

A similar dependence B_{hf} on the number of sp -atoms located in the second to fourth coordination shells is shown in Figure 1, *b*. In contrast to $B_{\text{hf}}(nn)$, no pronounced trend is observed here. You can see that the same number of atoms of sp -elements in the I coordination shell of Fe atom corresponds to different (maximum difference of ~ 30 T) HMF values B_{hf} . The reason for such spread is not only the variations of the number of Al and B atoms in II, III and IV coordination shells, but also the specific positions of those atoms within the cell.

A similar analysis conducted for isomer shift δ is presented in Figure 2, *a* for I coordination shell, and in Figure 2, *b* — for subsequent II–IV shells. The first shell demonstrates a clear trend to isomer shift increase with the increase in the number of sp -atoms. This dependence can be approximated by a linear function: when the quantity of Al and B sp -atoms in I coordination shell increases, the value of the isomer shift increases approximately by 0.02 mm/s per atom. The same result (slope of 0.02 mm/s) will be obtained, if we consider separately only binary

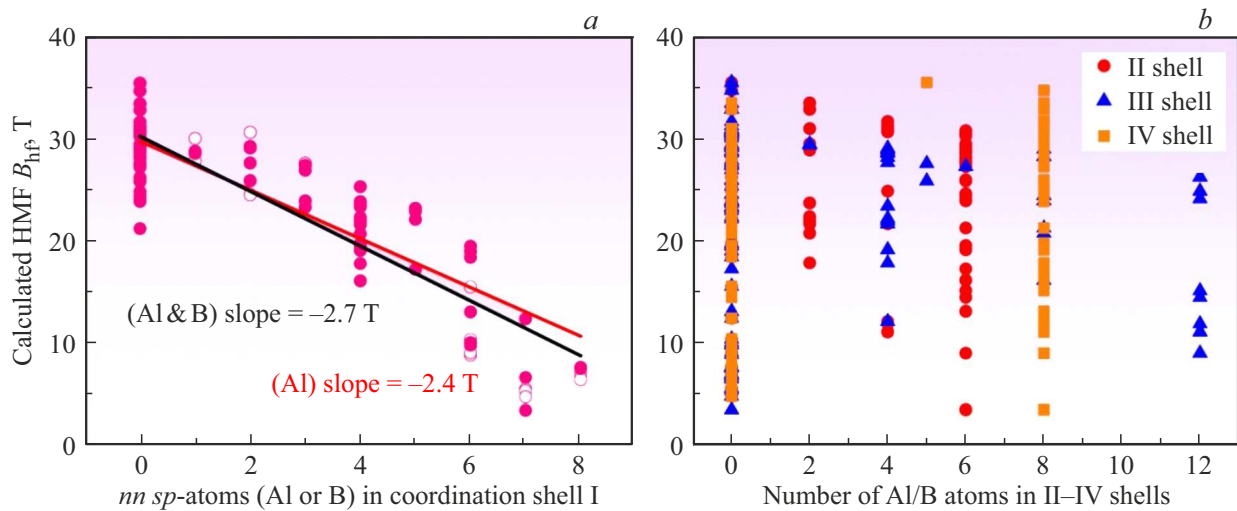


Figure 1. Dependence of the calculated HMF B_{hf} at the ^{57}Fe nucleus on the number of aluminum or boron atoms in I coordination shell (a); in II–IV shells (b).

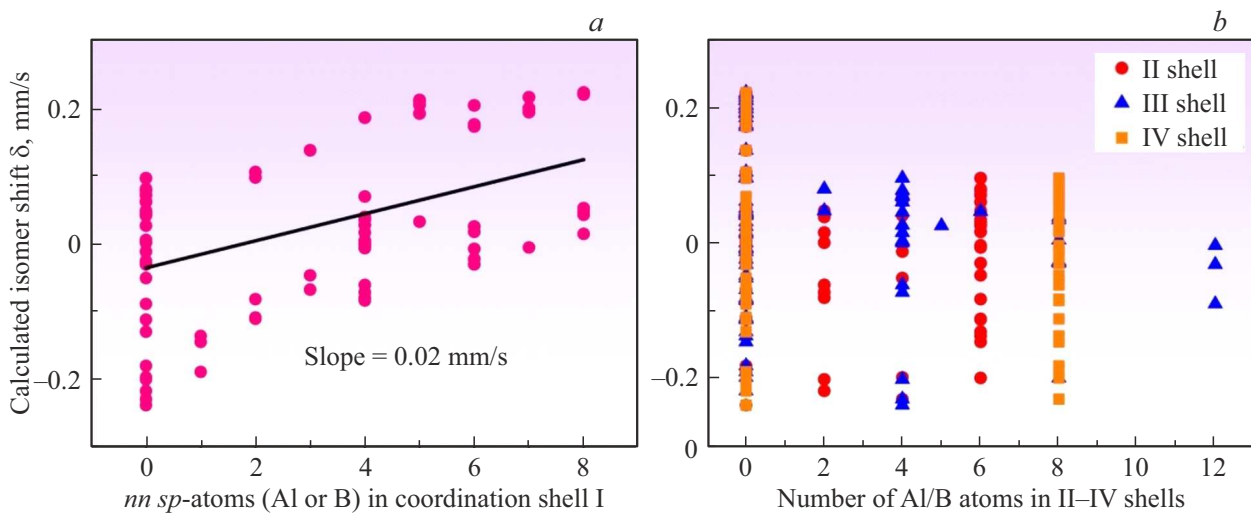


Figure 2. Dependence of the calculated value of isomer shift at the ^{57}Fe nucleus on the number of Al/B atoms in the first coordination shell (a); in II–IV shells (b).

Fe–Al systems (without boron). And this result also agrees with the data available for Fe–Al [13]. Therefore, each Al/B atom in the nearest environment of Fe atom results in reduction of HMF B_{hf} , and also to reduction in electron charge density, i.e. contact s -density at ^{57}Fe nucleus. From Figure 2, *b* you can see that similarly to $B_{\text{hf}}(nm)$, the values of isomer shift caused by replacement of Fe atom with sp -atom in II, III and IV coordination shells do not demonstrate a systemic dependence. It should be noted that absolute values of isomer shift in all cases remain within the limits of approximately from -0.2 to $+0.2$ mm/s, which contributes to rather high uncertainty, when these values are used in the experimental practice of Mössbauer effect. The average difference in ^{57}Fe values of HMF B_{hf} at the same of atoms in II, III and IV coordination shells reaches 2 T, absolute value

of isomer shift — 0.2 mm/s and magnetic moment — to $0.2 \mu_{\text{B}}$ /atom.

Thus, the present calculations show that, in the Fe–Al–B system (just as in the binary Fe–Al system [25]), a proper analysis of the magnetic state in terms of local atomic environments generally requires taking several nearest coordination shells into account. It is easy to do such analysis in alloys of stoichiometric composition ($c_{\text{Al}} + c_{\text{B}} = 25$ at.%), when the number of chemical and magnetic-nonequivalent configurations is small. In non-stoichiometric ordered or in disordered systems which contain an enormous variety of local environments around the Fe atom, it is necessary — besides calculating the hyperfine interaction parameters — to analyze the statistical weights of the individual local configurations. The example of such analysis is given further.

Table 1. Calculated values of the HFI parameters for some configurations of the nearest environment of Fe atom. A configuration is a shorthand notation that specifies the numbers of Al and B atoms in the first four coordination shells (explained in the text); P_{D03} — probability of this configuration for $D0_3$ type ordering; P_{A2} — probability of this configuration for A2 type ordering; B_{hf} — HMF, δ — isomer shift

Configuration	P_{D03} , %	P_{A2} , %	B_{hf} , T	δ , mm/s
[40 00 00 00]	0.9109	0.00189	25.4	0.184
[40 00 01 00]	0.8408	0.00174	—	—
[40 00 02 00]	0.3558	0.00074	—	—
[40 00 04 00]	0.0158	0.00003	23.4	0.000
[40 00 05 00]	0.0019	0.00000	—	—
[40 02 00 00]	0.0808	0.00017	23.8	-0.081
[40 04 00 00]	0.0005	0.00005	—	—
[40 00 00 80]	0.0000	0.00000	19.8	-0.085
[40 40 40 00]	0.0000	0.00000	21.7	0.068
[00 00 00 00]	0.0000	0.77088	32.9	0
[50 00 00 00]	0.2803	0.00012	23.2	0.210
[20 00 00 00]	0.0000	0.12771	29.2	-0.110
[10 00 00 00]	0.0000	0.47439	30.1	-0.190

3.2. Analysis of local atomic configurations

According to the X-ray diffraction and chemical analysis data, the $\text{Fe}_{65}\text{Al}_{30}\text{B}_5$ ternary alloy has $D0_3$ superlattice [15,16] and is non-stoichiometric. Therefore, to analyze the local atomic structure, it is natural to consider the statistic model of $D0_3$ type of ordering (spatial group $Fm\bar{3}m$). Let us calculate the probabilities of all local non-equivalent configurations for all variants of Fe, Al, B atom arrangement from I to IV coordination shell. For example, the probability of the configuration with 4 atoms of iron and 4 atoms of aluminum in I coordination shell — $P[40 \text{ RR RR RR}] \approx 37.611\%$ (the most probable configuration within I coordination shell); here „40“ means 4 aluminum atoms and 0 boron atoms in I shell, „RR“ — a random (statistical) occupancy of Al/B in II, III, IV coordination shells. Within the full ensemble „40“ the most probably configuration is $P[40 00 00 00] \approx 0.9109\%$. The second-most probable configuration (probability $P[40 00 10 00] = P[40 00 01 00] \approx 0.8408\%$) differs only by one atom (Al or B) in the third coordination shell and produces virtually the same HMF value at the ^{57}Fe nucleus. In any case, in other local configuration (from the set $P[40 \text{ RR RR RR}]$, the number of sp -atoms will be greater, and that means that HMF at nucleus Fe nucleus in these configurations will be smaller. Table 1 shows the calculated

probabilities and values of HMF B_{hf} and isomer shift δ for Fe atoms in some configurations of $D0_3$ -structure.

It is clearly seen that, with increasing number of Al (or B) atoms in the II, III, and IV coordination shells, the probability of such local environments decreases to zero for the given alloy composition, while the HMF changes only slightly (by $\sim 2\text{T}$). The conducted analysis brings us to the conclusion that for MS tasks of such ternary Fe–Al–B systems it is feasible to consider only the first coordination shell. At the same time, the contribution of other shells should be considered as 1) broadening of the corresponding contribution to the Mössbauer spectrum ($\sim 8\%$ of the values corresponding only to I shell); 2) minor shift towards smaller values of HMF ($\sim 3\%$ of the values corresponding only to I shell).

Analysis of Mössbauer spectra of $\text{Fe}_{65}\text{Al}_{30}\text{B}_5$ ordered alloy [15,16] showed that the alloy is not single-phase, and another possible phase is A2 phase with a random distribution of Fe, Al and B atoms over the sites of a bcc-lattice (α -Fe structure with the space group $Im\bar{3}m$). In this case a similar approach is used (see Table 1, P_{A2}). The most probable local configurations of Fe atom in A2 structure will be those that contain sp -elements only in the first coordination shell of the iron atom.

Therefore, from the entire volume of calculated HMF values (Figure 1, a) two distinct data arrays can be singled out, corresponding to: 1) ordered $D0_3$ -structure and 2) disordered A2-structure. Slopes of the approximating straight lines $B_{\text{hf}}(nn)$ for the specified structures differ and are as follows: 1) -2.9T/atom ; 2) -2.2T/atom .

Note that the HFI parameters calculated by DFT methods may not coincide exactly, in numerical terms, with the experimental values obtained, for example, from Mössbauer spectra. Nevertheless, it is the relative changes that are the key value and may successfully be used in analysis and interpretation of real Mössbauer spectra. Therefore, even though absolute values of calculated parameters do not always match the experiment precisely, trends and regularities revealed by the calculations prove to be highly useful and informative.

3.3. Estimation of the core and valence contributions to HMF

WIEN2k software package enables to separately analyze the contributions of various electron states to calculated values of HMF at ^{57}Fe nucleus. In particular, the software makes it possible to separate the contribution of valence electrons from the contribution of ion core electrons — „core“ or „inner“ electrons. Physically the internal states mean electron levels, whose wave functions are fully localized inside the *muffin-tin* sphere. These electron states are located at much lower energy levels (below $E = -6\text{Ry}$, which is a standard value in calculations of such Fe–Al systems), indicating their deep energy position and strong localization near the atom nucleus. And valence electrons possess higher energies and have wave functions that extend

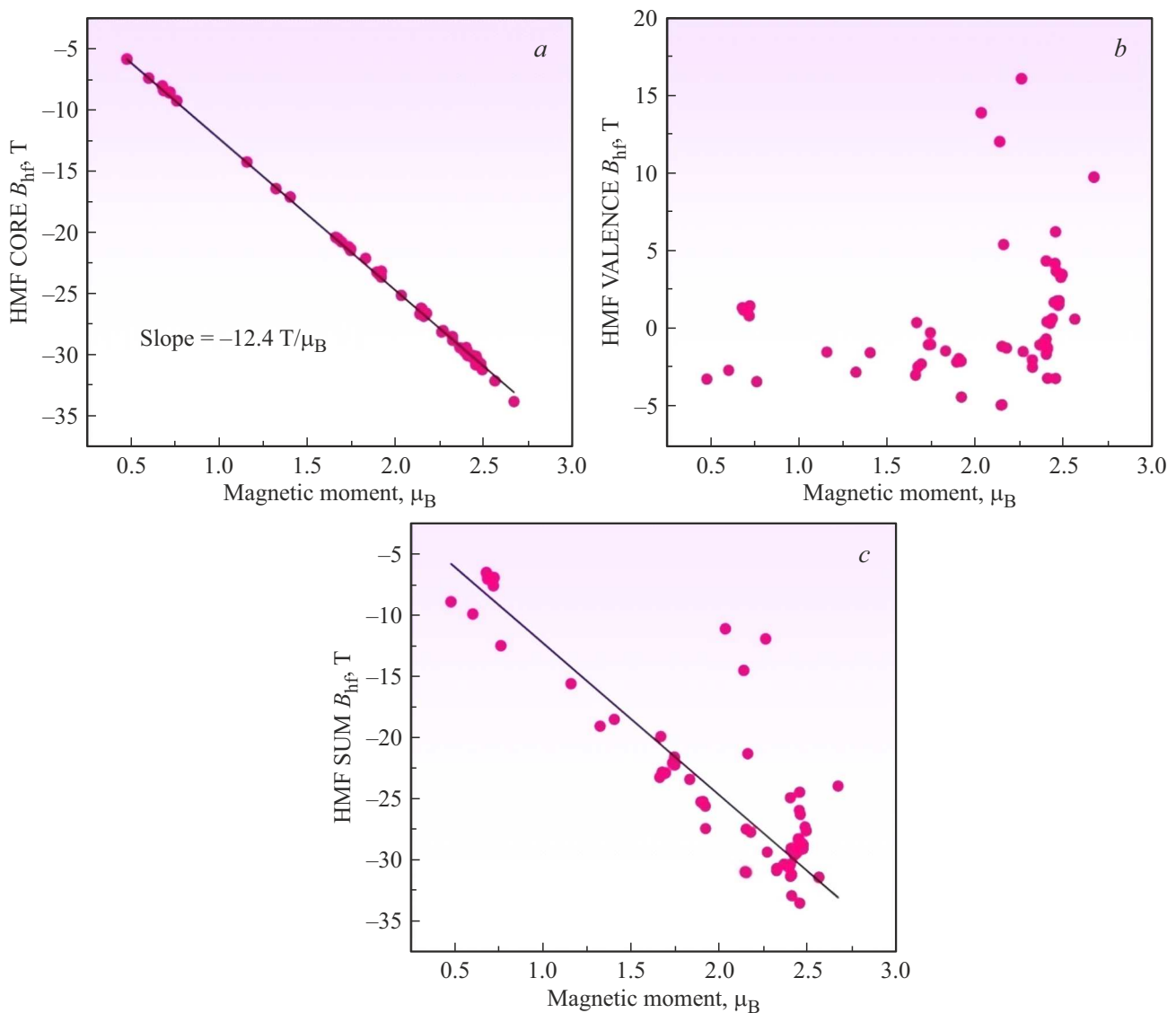


Figure 3. Dependence of the calculated value of hyperfine magnetic field at ^{57}Fe nuclei on magnetic moment in binary Fe–Al and ternary Fe–Al–B alloys: *a* — contribution of internal (core) electrons; *b* — contribution of external (valence) electrons; *c* — total contribution of both types of electron states.

beyond the *muffin-tin* sphere, reflecting the delocalized character of their state.

Figure 3 shows the dependence of the HMF value at the Fe nucleus on the value of the calculated magnetic moment for binary Fe–Al and ternary Fe–Al–B systems. The contribution of core electrons to HMF is given in Figure 3, *a*, and of valence ones — Figure 3, *b*; the total dependence B_{hf} on the magnetic moment on Fe atom is shown in Figure 3, *c*. The contribution of core electrons shows a clear linear dependence of HMF B^{core} on magnetic moment m_{Fe} , which is approximated by equation:

$$B^{\text{core}} = -A \cdot m_{\text{Fe}}, \quad (1)$$

where the coefficient of proportionality A is around $12.4 \text{ T}/\mu_B$, which agrees well with the known literature

data [26]. The obtained coefficient A may be used to analyze the magnetic microstructure using MS.

3.4. HMF calculations for a cell where B atom occupies an interstices

Boron atoms, due to their relatively small size (Figure 4), can be accommodated in the interstitial positions between the iron and aluminum lattice sites in the ternary alloys. Fe–Al–B. The situations of such interstitial arrangement of boron atoms were studied additionally. Two cases were considered: 1) $\text{Fe}_{11}\text{Al}_5\text{B}$ — presented in Figure 4, *a*; and 2) $\text{Fe}_{12}\text{Al}_4\text{B}$ — in Figure 4, *b*. The choice of such elementary cells was due their similarity in composition to the experimentally studied alloys [15,16]. The two configurations differ in that, in the first, the boron atom

Table 2. Calculated values of HFI parameters for systems $\text{Fe}_{11}\text{Al}_5$, $\text{Fe}_{11}\text{Al}_5\text{B}$, $\text{Fe}_{12}\text{Al}_4$, $\text{Fe}_{12}\text{Al}_4\text{B}$. N — corresponds to the number of iron atom in Figure 4; r — distance between the nearest iron atoms; δ — calculated value of isomer shift; B_{hf} — calculated value of HMF, which is a sum of „core“ and valence contributions taken by the module; core — contribution to HMF from internal „core“ electrons; val — contribution to HMF from „external“ valence electrons

N	$\text{Fe}_{11}\text{Al}_5$					$\text{Fe}_{11}\text{Al}_5\text{B}$				
	r , Å	δ , mm/s	B_{hf} , T	core, T	val, T	r , Å	δ , mm/s	B_{hf} , T	core, T	val, T
1	2.50	0.06	29.0	-30.7	1.8	2.618	0.12	27.6	-31.2	3.6
2	2.50	0.06	29.0	-30.7	1.8	2.558	0.14	31.4	-32.1	0.7
3	2.50	0.21	23.1	-20.1	-3.0	2.618	0.24	19.9	-20.4	0.5
4	2.50	0.21	23.1	-20.1	-3.0	2.540	0.22	21.6	-21.5	-0.1
N	$\text{Fe}_{12}\text{Al}_4$					$\text{Fe}_{12}\text{Al}_4\text{B}$				
	r , Å	δ , mm/s	B_{hf} , T	core, T	val, T	r , Å	δ , mm/s	B_{hf} , T	core, T	val, T
5	2.496	0.06	31.0	-29.9	-1.1	2.578	0.09	28.7	-30.3	1.6
6	2.496	0.06	31.0	-29.9	-1.1	2.455	-0.00	25.4	-21.4	-4.0
7	2.496	0.06	31.0	-29.9	-1.1	2.540	0.13	34.6	-31.9	0.3
8	2.496	0.19	25.0	-23.4	1.6	2.578	0.24	21.0	-21.7	0.7
9	2.496	0.19	25.0	-23.4	-1.6	2.455	0.18	24.0	-25.1	1.1

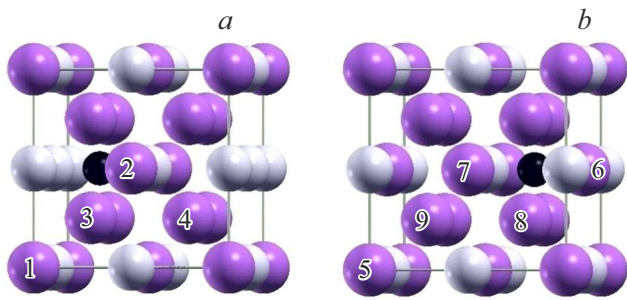


Figure 4. Unit cells $\text{Fe}_{11}\text{Al}_5\text{B}$ (a) and $\text{Fe}_{12}\text{Al}_4\text{B}$ (b). Non-equivalent positions of iron atoms are numbered, and their HFI parameters are specified in Table 2. The boron atom occupying an interstitial site is shown as a black sphere. Purple is for Fe, and grey — for Al.

is coordinated by four Fe atoms and two Al atoms, whereas in the second case its nearest environment contains five Fe atoms and one Al atom. Formation enthalpy for these systems was estimated using the scheme described in paper [27]. The calculations demonstrated that both systems are stable and energetically favorable: enthalpy of formation for the first system is -0.29 eV/atom, and for the second one — -0.37 eV/atom.

The systems chosen to compare calculated values of HFI parameters (δ and B_{hf}) in $\text{Fe}_{11}\text{Al}_5\text{B}$, $\text{Fe}_{12}\text{Al}_4\text{B}$ cells were $\text{Fe}_{11}\text{Al}_5$ and $\text{Fe}_{12}\text{Al}_4$ (without boron as the interstitial atom). It is known that the main contribution to ^{57}Fe B_{hf} at the iron nucleus comes from the core (inner-shell) electrons. It is also known that the interatomic spacing of iron affects the magnitude of the magnetic moment, which in turn influences the contribution of the inner electrons to the hyperfine magnetic field. As interatomic distances increase, there is a growth of contribution of

„core“ electrons to HMF, provided for by spin polarization of internal s -levels with d -electrons. This behavior is typical for Fe- sp -element systems (for example, Fe-Al, Fe-Si) [28]. Insertion of B atom into the an interstitial site of the crystal lattice Fe-Al enlarges the spacing between neighbouring atoms, which in turn modifies the hyperfine magnetic field contributed by the core electrons. However, in contrast to the defect-free Fe- sp -element systems, the interstitial placement of an atom requires accounting for the valence-electron contribution to the hyperfine magnetic field; in this case, that contribution is positive and dominates the overall HMF. The calculations show that inserting a single boron atom into an interstitial site in either system lowers the average value of HMF approximately by 10%, mainly due to the contribution from valence electrons. Besides, in the systems under study, iron atoms are found (in some positions), for which the HMF increases due to both core and valence electrons (see Table 2, $N2$). However, the cause for such behavior remains unclear and requires a deeper future analysis beyond the current study.

4. Conclusion

Quantum-mechanical calculations of hyperfine interaction parameters (hyperfine field at ^{57}Fe nucleus and isomer shift) for the ternary Fe-Al-B system show that the local HFI parameters to a large extent depend on the number of Al and B atoms in the first coordination shell of Fe atom and the specific position occupied by sp -atom in the unit cell. Substitution of Fe atoms for Al or B causes linear reduction of HMF approximately by 2.7 T per each atom, and also increase of isomer shift by 0.02 mm/s. Impact of substitution of Fe for sp -atom in the more distant coordination shells of Fe atom is noticeable, yet it shows no clear trend. Applying Mössbauer spectroscopy models

that consider only the nearest-neighbor environment of iron atoms requires evaluating the statistical weight of the various local Fe configurations. The considered case of $D0_3$ -ordered $\text{Fe}_{65}\text{Al}_{30}\text{B}_5$ alloy showed that the influence of II–IV shells appeared as a minor correction that slightly broadens the Mössbauer line ($\sim 8\%$) and shifts HMF toward lower values ($\sim 3\%$).

An analysis of the core- and valence-electron contributions to HMF at ^{57}Fe nucleus has shown that the magnitude of the hyperfine magnetic field is proportional to the magnetic moment of the core electrons, with a proportionality coefficient of about $12.4\text{ T}/\mu_{\text{B}}$, whereas the valence electrons display no pronounced correlation.

Using the $\text{Fe}_{11}\text{Al}_5\text{B}$ and $\text{Fe}_{12}\text{Al}_4\text{B}$ systems as test cases, we investigated whether boron atoms can occupy interstitial positions in the crystal lattice and how this affects the HFI parameters. Boron can stably occupy interstitial sites in $\text{Fe}_{11}\text{Al}_5\text{B}$ and $\text{Fe}_{12}\text{Al}_4\text{B}$ (calculated value of enthalpy of formation -0.29 and -0.37 eV/atom); its presence expands the lattice and induces a positive valence contribution to the HMF. This causes a reduction in the average HMF approximately by 10% relative to defect-free alloys Fe–Al. Quantum-mechanical calculations of hyperfine parameters are essential for the accurate interpretation of Mössbauer spectra when investigating the magnetic microstructure of complex systems with structural and magnetic inhomogeneities.

Conflict of interest

The authors declare that they have no conflict of interest.

References

- [1] Special Issue Discussion Meeting on the Development of Innovative Iron Aluminium Alloy Ed. by D.G. Morris. *Intermetallics* **13**, 12, 1255 (2005). <https://doi.org/10.1016/j.intermet.2004.08.011>
- [2] Special Issue Materials Science and Engineering A. *Mater. Sci. Eng. A* **258**, 1–2, 1 (1998). [https://doi.org/10.1016/S0921-5093\(98\)00908-3](https://doi.org/10.1016/S0921-5093(98)00908-3)
- [3] C. Bormio-Nunes, M.B. Dias, L. Ghivelder. *J. Alloys Compd.* **574**, 467 (2013). <https://doi.org/10.1016/j.jallcom.2013.05.122>
- [4] C. Bormio-Nunes, O. Hubert. *JMMM* **393**, 404 (2015) <https://doi.org/10.1016/j.jmmm.2015.05.091>
- [5] A. Hernando, X. Amils, J. Noguez, S. Surinach, M.D. Baro, M.R. Ibarra. *Phys. Rev. B* **58**, R11864 (1998). <https://doi.org/10.1103/PhysRevB.58.R11864>
- [6] E.P. Elsukov, E.V. Voronina, A.S. Shuravin, A.V. Zagaynov, A.V. Korolev, S.K. Godovikov, E.A. Pechina, A.E. Elsukova. *FMM* **102**, 1, 733 (2006). (in Russian). <https://doi.org/10.1134/S0031918X06070076>
- [7] F. Plazaola, E. Apinaniz, D.M. Rodriguez, E. Legarra, J.S. Garitaonandia. In *Advanced Magnetic Materials* ed. by Leszek Malkinski. InTech. (2012). pp. 133–170. <https://doi.org/10.5772/2298>
- [8] E. Apinaniz, F. Plazaola, J.S. Garitaonandia. *Eur. Phys. J. B* **31**, 167 (2003). <https://doi.org/10.1140/epjb/e2003-00021-y>
- [9] F. Lechermann, F. Welsch, C. Elsasser, C. Ederer, M. Fahnle, M. Sanchez, B. Meyer. *Phys. Rev. B* **65**, 132104 (2002). <https://doi.org/10.1103/PhysRevB.65.132104>
- [10] Y.H. Liu, X.Y. Chong, Y.H. Jiang, R. Zhou, J. Feng. *Physica B Condens. Matter* **503**, 10 (2016). <https://doi.org/10.1016/j.physb.2016.10.032>
- [11] B.V. Reddy, S.C. Deevi, F.A. Reuse, S.N. Khanna. *Phys. Rev. B* **64**, 132408 (2001). <https://doi.org/10.1103/PhysRevB.64.132408>
- [12] J.P. Das, B.K. Rao, P. Jena, S.C. Deevi. *Phys. Rev. B* **66**, 184203 (2002). <https://doi.org/10.1103/PhysRevB.66.184203>
- [13] M.B. Stearns. *J. Appl. Phys.* **35**, 1095 (1964). <https://doi.org/10.1063/1.1713394>
- [14] D.R. Noakes, A.S. Arrott, M.G. Belk, S.C. Deevi, Q.Z. Huang, J.W. Lynn, R.D. Shull, D.Wu. *Phys. Rev. Lett.* **91**, 217201 (2003). <https://doi.org/10.1103/PhysRevLett.91.217201>
- [15] E.V. Voronina, A.K. Arzhnikov, A.I. Chumakov, N.I. Chistyakova, A.G. Ivanova, A.V. Pyataev, A.V. Korolev. *Adv. Cond. Matter Phys.* **2018**, 5781873 (2018). <https://doi.org/10.1155/2018/5781873>
- [16] E.V. Voronina, A.G. Ivanova, A.K. Arzhnikov, A.I. Chumakov, N.I. Chistyakova, A.V. Pyataev, A.V. Korolev. *Phys. Solid State* **60**, 4, 730 (2018). <https://doi.org/10.1134/S1063783418040340>
- [17] A.K. AlSaedi, A.G. Ivanova, E.V. Voronina, A.K. Arzhnikov. *Metall. Mater. Trans. A* **51**, 10, 5365 (2020). <https://doi.org/10.1007/s11661-020-05938-3>
- [18] Y. Cheng, Z.L. Lv, X.R. Chen, L.C. Ca. *Comput. Mater. Sci.* **92**, 253 (2014). <https://doi.org/10.1016/j.commatsci.2014.05.048>
- [19] A. Kellou, H.I. Feraoun, T. Grosdidier, C. Coddet, H. Aourag. *Acta Mater.* **52**, 3263 (2004). <https://doi.org/10.1016/j.actamat.2004.03.023>
- [20] J.M. Raulot, A. Fraczkiwicz, T. Cordonnier, H. Aourag, T. Grosdidier. *J. Mater. Sci.* **43**, 3867 (2008). <https://doi.org/10.1007/s10853-007-2338-7>
- [21] A.F. Abdullin, E.V. Voronina. *Magn. Reson. Solids* **27**, 25101 (2025). <https://doi.org/10.26907/mrsej-25101>
- [22] P. Blaha, K. Schwarz, G.K.H. Madsen, D. Kvasnicka, J. Luitz, R. Laskowski, F. Tran, L.D. Marks. *WIEN2k An Augmented Plane Wave + Local Orbitals Program for Calculating Crystal Properties Software*. 2018.
- [23] P. Blaha, K. Schwarz, F. Tran, R. Laskowski, G.K.H. Madsen, L.D. Marks. *J. Chem. Phys.* **152**, 074101 (2020). <https://doi.org/10.1063/1.5143061>
- [24] J.P. Perdew, K. Burke, M. Ernzerhof. *Phys. Rev. Lett.* **77**, 3865 (1996). <https://doi.org/10.1103/PhysRevLett.77.3865>
- [25] A.K. Arzhnikov, L.V. Dobysheva. *FTT* **50**, 11, 2009 (2008). (in Russian).
- [26] D. Kaptas, E. Svab, Z. Somogyvari, G. Andre, L.F. Kiss, J. Balogh, L. Bujdoso, T. Kemény, I. Vincze. *Phys. Rev. B* **73**, 012401 (2006). <https://doi.org/10.1103/PhysRevB.73.012401>
- [27] E.V. Voronina, A.F. Abdullin, A.G. Ivanova, L.V. Dobysheva, A.V. Korolev, A.K. Arzhnikov. *JETP* **136**, 89 (2023). <https://doi.org/10.1134/S1063776123010120>
- [28] A.J. Freeman, R.E. Watson. In *Magnetism Vol. IIB* Ed. by G.T. Rado H. Suhl. Academic Press, N. Y. (1965). pp. 167

Translated by M.Verenikina